Persistent Dentate Granule Cell Hyperexcitability after Neonatal Infection with Lymphocytic Choriomeningitis Virus

Bradley D. Pearce,[1] Scott C. Steffensen,[2] Alyssa D. Paoletti,[2] Steven J. Henriksen,[2] and Michael J. Buchmeier[2]

[1]*Emory University School of Medicine, Department of Psychiatry, Atlanta, Georgia 30322, and*
[2]*The Scripps Research Institute, Department of Neuropharmacology, La Jolla, California 92037*

Infection of neonatal Lewis rats with lymphocytic choriomeningitis virus (LCMV) produces distinct retinal, cerebellar, and hippocampal neuropathology. To understand the neurophysiological consequences of LCMV-induced hippocampal pathology, we studied evoked monosynaptic potentials and electroencephalographic (EEG) activity in the dentate gyrus and CA1 and CA3 subfields of the hippocampus *in vivo*. Lewis rats were inoculated intracerebrally with LCMV at postnatal day 4. In rats studied 84–107 d postinfection, virus was cleared from the dentate gyrus and the number of dentate granule cells was decreased by 70%. No viral antigen or cell loss was apparent in CA1 or CA3. The hippocampal EEG of LCMV-infected rats 84–102 d postinfection was dominated by continuous theta. Although evoked potentials elicited in CA1 and CA3 by monosynaptic afferent stimulation revealed no differences between sham- and LCMV-infected rats, there was a site-specific dissociation of synaptic [population excitatory postsynaptic potential (pEPSP)] and cellular (population spike) responses and a suppression of GABA-mediated recurrent inhibition in the dentate gyrus of LCMV-infected rats. These findings indicate that GABA-mediated inhibition was markedly decreased in LCMV-infected rats. In support of this, parvalbumin-immunoreactive cell bodies and neuronal processes were decreased in LCMV-infected rats, suggesting that a subpopulation of GABA interneurons was affected. These findings indicate that abnormalities in synaptic function persist after clearance of infectious virus from the central nervous system and suggest that decreased inhibition subsequent to pathological sequelae in a subpopulation of GABA interneurons may be implicated in the hyperexcitability of dentate granule cells.

Key words: LCMV; hippocampus; GABA; recurrent inhibition; theta rhythm; excitotoxicity

Hippocampal pathology has been described in several human disorders having neurodevelopmental components, including schizophrenia (Bogerts, 1993), autism (Bauman, 1991), and temporal lobe epilepsy (Houser, 1990). It has been hypothesized that a viral insult during embryogenesis or development may be involved in the etiology of these disorders. Supporting this hypothesis are epidemiological studies (Deykin and MacMahon, 1979; Kirch, 1993) and the known teratogenic potential of viruses (Prober and Arvin, 1987) that can preferentially infect dividing neuroblasts (Margolis and Kilham, 1975), disrupt neural cell migration (Stoltenburg et al., 1991), or inhibit developmentally regulated hormone production (Oldstone et al., 1984). The complex inter-relationship between neuronal circuitry and neuron degeneration (Houser, 1990; Olney et al., 1991) suggests that viruses can induce neuronal death through an indirect mechanism, for example, by interrupting inhibitory control over a potentially excitotoxic synapse. Such a mechanism would imply that a viral insult early in development could initiate a pathological cascade that would continue even after the virus had been cleared. The rat hippocampus provides a useful model system for examining virus-induced changes in neuronal circuitry, because it is a target of several known viruses (Monjan et al., 1973b; Narayan et al., 1983; Parham et al., 1986) and its electrophysiological parameters are well established.

In neonatal rats, a distinct pattern of lymphocytic choriomeningitis virus (LCMV) infection is observed in which cells undergoing division at the time of inoculation are preferentially infected. Thus, in the brains of neonatal rats 13–17 d after LCMV infection, there are numerous infected cells observed in the cerebellum, olfactory bulb, and dentate gyrus of the hippocampus (Monjan et al., 1973a, 1975; Baldridge et al., 1993). The pathology in the cerebellum is complete by 21 d postinfection and is immune-mediated, whereas degeneration of neurons in the dentate gyrus develops over months and progresses even after the virus is apparently cleared (Monjan et al., 1974, 1975). The mechanism underlying the degeneration in the dentate gyrus is unknown. Excitotoxic mechanisms deserve consideration because activation of excitatory amino acid receptors is known to cause neurodegeneration in the hippocampus (Nadler et al., 1978), and in measles virus-infected mice, the *N*-methyl-D-aspartate (NMDA) antagonist MK-801 protects CA1 hippocampal neurons from damage attributable to encephalitis (Andersson et al., 1993).

Although the behavioral abnormalities observed after LCMV infection implicate the limbic system (Monjan et al., 1975), the effects of virus infection on hippocampal function at the cellular or electrophysiological level have not been described. In the present study we examined the long-term sequela of neonatal LCMV infection on hippocampal circuitry in rats. In addition, we

Received July 13, 1995; revised Sept. 19, 1995; accepted Sept. 25, 1995.

This work was supported by Public Health Service Grants NS12428 and AI16102 to M.J.B. B.P. was supported by NIMH training Grant MH19185. We thank Drs. Floyd Bloom and Andrew Miller for help with reading the slides and for the quantitation of sections, respectively. We thank Drs. Michael Wilson, Lisa Gold, and Howard Fox for critical reading of the manuscript. We also thank Drs. Jory Baldridge and Tanya McGraw for help in developing the LCMV neonatal rat model.

Correspondence should be addressed to Michael J. Buchmeier, Ph.D., Department of Neuropharmacology (CVN-8), The Scripps Research Institute, 10666 N. Torrey Pines Road, La Jolla, CA 92037.

evaluated the effects of MK-801 on LCMV-induced abnormalities in hippocampal function.

MATERIALS AND METHODS

Subjects and surgical preparation. Lewis rat pups on postnatal day 4 were infected by intracerebral inoculation of 1000 plaque-forming units of Armstrong 4 LCMV, as described previously (Baldridge et al., 1993). Sham-infected controls received an equivalent injection volume of vehicle. All rats were weaned (three to four animals per cage) on postinfection day 19. Electrophysiological studies and quantitative assessments of cell loss were performed exclusively on male rats because this allowed for more consistent electrode placement. In studies examining viral clearance, both males and females were included in the analysis. On postinfection day 20, four LCMV-infected and four sham-infected animals were administered MK-801 0.1 $mg \cdot kg^{-1} \cdot d^{-1}$ in their drinking water. Initially, MK-801 was added to the drinking water at a concentration of 0.001 mg/ml and was adjusted every 3 d to account for changes in body weight and fluid consumption. Electrophysiological studies were performed on male animals between postinfection days 84 and 102. Subjects (250–350 gm) were anesthetized with halothane (3.0–4.0%) and placed into a stereotaxic apparatus. Body temperature was monitored and maintained at 37.0 ± 0.1°C by a feedback-regulated heating pad. The skull was exposed and holes were drilled to accommodate placement of stimulating and recording electrodes. The dura was opened over recording sites to prevent breakage of micropipettes. Halothane anesthesia was maintained at 0.75% after surgery.

Immunohistochemistry. Staining for LCMV viral antigen was performed on paraffin-embedded sections as described previously (Baldridge et al., 1993), using a polyclonal guinea pig anti-LCMV antibody, followed by a biotinylated secondary antibody, ABC reagent (Vector Laboratories, Burlingame, CA), and diaminobenzidine.

For Nissl and parvalbumin staining, rats were prepared by transcardiac perfusion with 120 ml of ice-cold PBS followed by 180 ml of 4% *p*-formaldehyde. After the perfusion, brains were removed and bisected sagittally. The left side of the brain was immersion-fixed in 1% *p*-formaldehyde for 24 hr at 4°C, cryoprotected by immersion in 20% sucrose, and then frozen at −70°C until sectioned for parvalbumin staining. The right side was immersion-fixed in Z-Fix (Analtech, Newark, DE) for 24 hr and paraffin-embedded; sagittal sections (3 μm thick) were taken for Nissl staining.

Coronal sections (15 μm thick) were used for parvalbumin staining. Sections for controls were taken from 3.5–5.0 mm posterior to bregma and sections for LCMV-infected rats were taken from 3.6–4.6 mm. Parvalbumin immunostaining was performed on slide-mounted frozen sections that were hydrated in Tris-buffered saline (TBS) (0.05 M Tris, 0.56% w/v NaCl) and permeabilized in TBS containing 1% Triton X-100 for 15 min. After incubation with 1% hydrogen peroxide to block endogenous peroxidase activity, and incubation with 10% normal goat serum (NGS), sections were treated with an antiparvalbumin monoclonal antibody (PA-235, Sigma, St. Louis, MO) diluted 1:1000 in TBS containing 1% NGS for 2.5 hr at 25°C. The reaction was completed using a rat-adsorbed biotinylated secondary antibody followed by ABC reagent and diaminobenzidine (Vector Laboratories).

Cell quantitation. For quantitation of neuronal loss, 3-μm-thick sagittal sections were taken from each brain at 1.7–1.9 mm lateral to the midline. A representative Nissl-stained section from each brain was scanned by video microscopy for quantitative assessment using National Institutes of Health IMAGE software. Computer-assisted counts of neuronal nuclei, identified by size and morphology, were performed on each scanned image. Dentate granule cells of the external limb (lying within the curve of Ammon's horn) and the internal limb (lying nearer the thalamus) were counted separately.

Cells staining for parvalbumin were counted visually in the dorsal hippocampus from a magnified (200×) image of one-to-two immunostained sections per brain. Parvalbumin-positive cells were defined as those cells with a stained cross-sectional area at least as large as the area of a dentate granule cell nucleus. For the purposes of quantitation, the dentate regions were demarcated by an imaginary line drawn from the lower border (suprathalamic edge) of the hippocampus, connecting the tips of each limb and terminating at the level of the hippocampal fissure. This region included the dentate molecular and granule layers as well as the hilus; however, parvalbumin-positive cells in the CA3c pyramidal cell layer in the hilus were not counted. Parvalbumin-positive cells in the hippocampus proper (CA1–CA3) were counted in the same sections and reported as a separate value because this region was consistently spared infection. Statistical differences between groups were evaluated using a two-tailed *t* test.

Extracellular recordings. Extracellular-evoked field potentials were recorded by single 3.0 M NaCl-filled micropipettes (5–10 MΩ; 1–2 μm inner diameter). Microelectrodes were stereotaxically oriented into the dentate gyrus (coordinates: 4.0 mm AP, 2.5 mm L, 2.8–3.1 mm V), hippocampus regio superior (4.0 mm AP, 2.5 mm L, 1.8–2.5 mm V), and hippocampus regio inferior (4.0 mm AP, 4.0 mm L, 3.0–3.5 mm V). Hippocampal electroencephalographic (EEG) and evoked responses were filtered at 0.1–50 Hz and 0.1 Hz to 10 kHz (−3 dB), respectively. Responses were displayed on Tektronix analog and digital oscilloscopes. EEG frequency spectra were generated from 4 sec epochs by fast Fourier transform digital signal processing algorithms. Extracellular potentials were digitized with National Instruments data acquisition boards at 200 Hz for EEG activity and 20 kHz for evoked responses (12-bit resolution). Analysis and processing of data on- and off-line were performed by customized National Instruments LabVIEW software on Macintosh Quadra computers.

Stimulation. Square-wave pulses (50–1000 μA; 0.15 msec duration; average frequency = 0.05 Hz) were generated by a constant-current isolation unit coupled to a Grass S88 stimulator and triggered by a MASTER-8 pulse generator or by computer. Field potentials were elicited in the dentate gyrus, hippocampus regio superior, or hippocampus regio inferior by stimulation of the perforant path (for recordings in dentate gyrus) or commissural pathway (for recordings in CA1 and CA3) with insulated, bipolar stainless steel (130 μm) electrodes located in the angular bundle (coordinates: 8.1 mm AP, 4.2 mm L, 3.0 mm V) or contralateral CA3 hippocampus (coordinates: 4.0 mm AP, 3.3 mm L, 2.8–3.2 mm V), respectively.

Stimulation of the perforant path elicited population excitatory postsynaptic potentials (pEPSPs) when recorded from the stratum moleculare of the dentate gyrus. pEPSP slopes were measured between 20 and 80% of the peak amplitude of the initial falling phase of the waveform. Recordings made from the cellular levels of the dentate gyrus, CA1, or CA3 yielded a population spike (PS) superimposed on the positive-polarity pEPSP/IPSP. PS amplitudes were determined by a median filter and peak detection algorithm. Stimulus–response curves were generated at selected afferent stimulus levels, and paired-pulse curves were tested at various intervals (0.010–10.0 sec) of orthodromic paired stimuli.

Analysis of responses. Three trials were averaged at each stimulus level of the stimulus–response curves and for each interval of the paired-pulse curves. Results for sham- and LCMV-infected groups were derived from calculations performed on animal weight, evoked field potential, paired-pulse, and EEG spectral analysis data and are expressed as mean ± SEM. Subsequent results were compared using the two-tailed *t* test at each point.

RESULTS

Localization of viral antigen and quantitation of cell loss in the dentate granule layer

In the hippocampus of rats infected with LCMV as neonates, a large portion of cells in the dentate gyrus was positive for viral protein as assessed by immunostaining at 15 d after infection (Fig. 1*B,D*). Cells staining for virus appeared more often in the internal limb than in the external limb of the dentate gyrus. Uninfected controls showed only minimal background staining (Fig. 1*A,C*). Ammon's horn apparently was spared infection, as reported previously (Monjan et al., 1973a; Baldridge et al., 1993). Immunostaining revealed viral antigen in cells of the dentate granule layer at 21 and 41 d postinfection. Viral antigen staining diminished in intensity and frequency over time and was virtually absent by 60–107 d postinfection (Fig. 1*F*). In a total of 23 sections from seven brains taken at various times during this late period after infection, antigen was detected in the hippocampi of only one brain. This brain was taken at 88 d postinfection and had only one to two antigen-containing cells per section in the dentate granule cell layer. Cell loss in the dentate granule layer was evident in all sections examined.

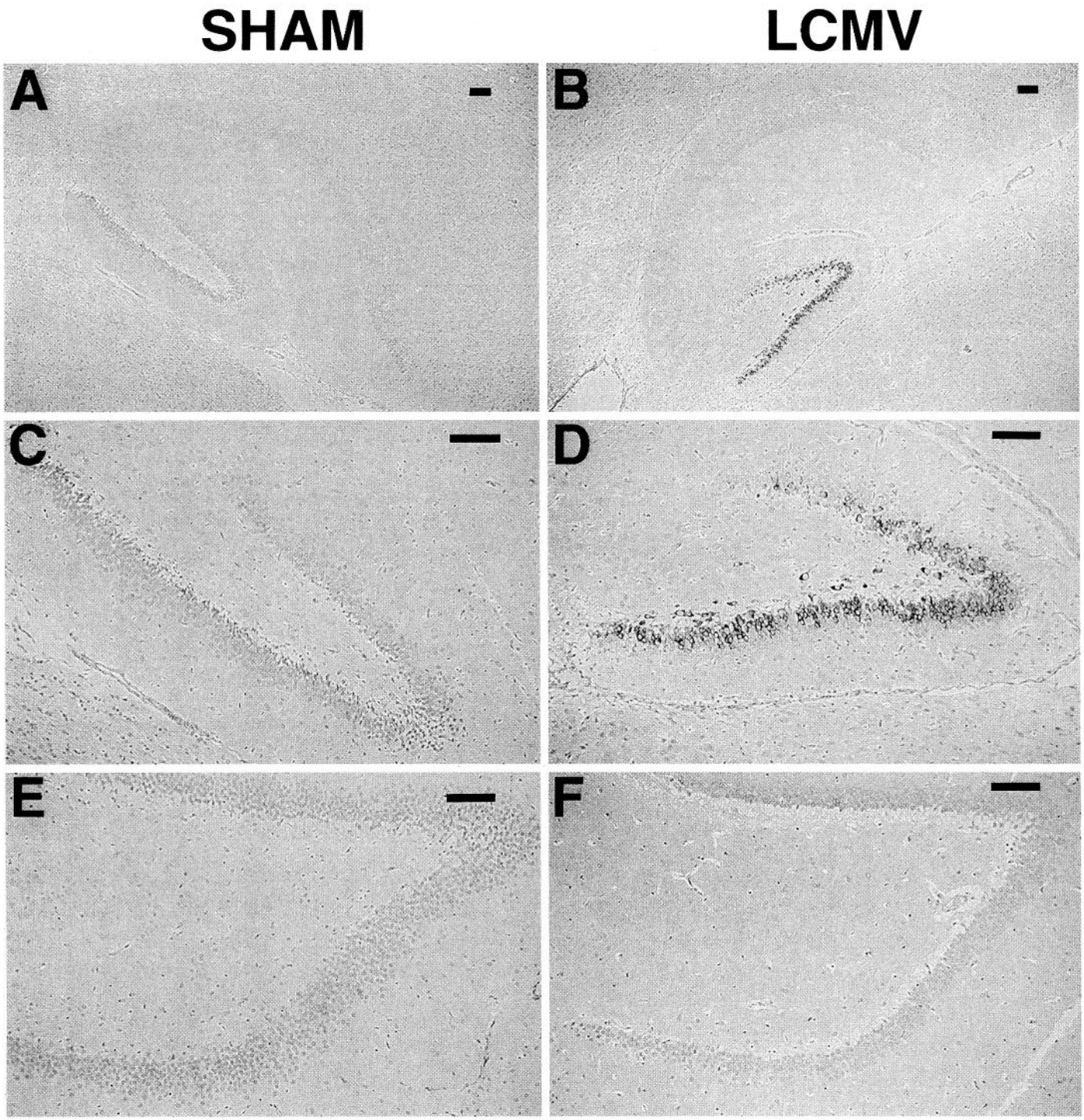

Figure 1. Clearance of LCMV protein and loss of granule cells in the dentate gyrus. Immunohistochemistry was performed by using a polyclonal antibody against LCMV. The dense-staining cells contain viral antigen proteins. *B*, In the hippocampus 15 d after neonatal infection with LCMV, numerous immunostained cells were evident (4× magnification). *D* is a higher magnification of *B* (10× magnification); compare with the background staining in the sham-infected control (*A, C*). *F*, At 88 d postinfection, LCMV staining was absent from LCMV-infected rats, and loss of dentate granule cells was evident. Compare with sham-infected controls (*E*). Scale bars, 100 μm.

To assess the magnitude of cell loss in the adult rats, we counted cells in the dentate granule layer in Nissl-stained sections from rats sampled between 79 and 87 d postinfection (Fig. 2). The loss in the external limb was 74.5%, whereas the loss in the internal limb was 67.5%.

Evoked potentials

We compared stimulus-evoked field potentials elicited in the dentate gyrus and the CA1 and CA3 hippocampus of LCMV-infected rats with those obtained from sham-infected controls. Stimulation of the perforant path (dentate) or commissural input

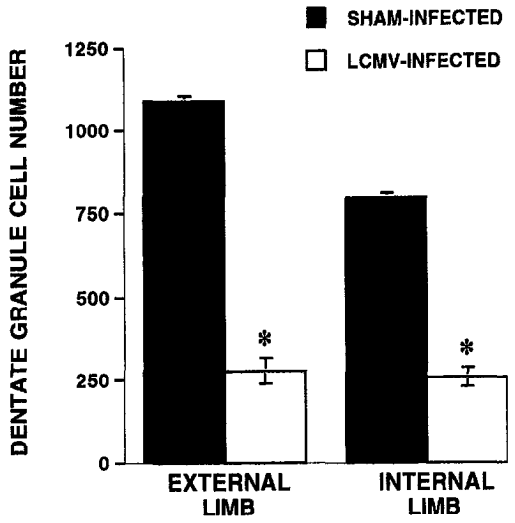

Figure 2. Loss of granule cells in the dentate gyrus in LCMV-infected rats. Neuronal nuclei in the internal and external limbs of the dentate granule cell layer of the dorsal hippocampus were counted from 3-μm-thick Nissl-stained sections taken from sham-infected and LCMV-infected rats at 79–86 d postinfection. Counts represent Nissl-stained nuclei per section for each limb of the dentate gyrus (n = 4 for LCMV-infected rats and n = 3 for sham-infected controls).

(CA1, CA3) produced a negative-going pEPSP recorded in the dendritic layer and negative-going PS superimposed on the positive-going pEPSP recorded in the cellular layer. The amplitude of the PS and the slope of the dendritic pEPSP increased monotonically with stimulus intensity. In the dentate gyrus, LCMV-infected PS amplitudes were slightly increased ($p < 0.02$; n = 9 at 50% stimulus level), and pEPSP slopes were markedly decreased ($p < 0.001$; n = 8) across all PS stimulus levels compared with sham-infected controls (Fig. 3*A*,*B*). To evaluate potential differences in dentate gyrus input/output coupling, we compared the slopes of the pEPSP/PS (E–S) curves between sham-infected and LCMV-infected animals. The slope of the dentate LCMV-infected E–S curve (3.35 ± 0.72; Fig. 3*C*; pEPSP slopes were taken at threshold, 50% maximum, and maximum PS levels) was significantly greater than that of sham-infected controls (1.37 ± 0.17; $p < 0.05$). There was no significant difference in evoked potentials between sham-infected and LCMV-infected animals in either the CA1 (PSs: 6.0 ± 0.1 mV vs 6.1 ± 0.2 mV; pEPSPs: 3.0 ± 0.2 mV/msec vs 3.0 ± 0.1 mV/msec; 50% maximum; $p > 0.05$; n = 9) or the CA3 (PSs: 5.5 ± 0.5 mV vs 5.8 ± 0.5 mV; pEPSPs: 2.9 ± 0.2 mV/msec vs 2.8 ± 0.1 mV/msec; 50% maximum; $p > 0.05$; n = 5) hippocampal subfields.

Recurrent inhibition

Equipotent paired-orthodromic stimulation of monosynaptic inputs to the dentate gyrus, CA1, or CA3 elicited triphasic and biphasic test/conditioning–response curves. In the dentate gyrus, paired-pulse curves were characterized by an early phase of absolute inhibition at interstimulus intervals (ISIs) <40 msec, moderate potentiation between 40 and 160 msec ISIs, and a late phase of relative inhibition from 160 to 2060 msec ISIs (Fig. 4*A*). In CA1, only two phases of paired-pulse responses were observed: an early phase of absolute inhibition at ISIs <160 msec and a late phase of moderate potentiation from 160 to 3060 msec (Fig. 4*B*). Paired-pulse responses in CA3 were biphasic, similar to those in CA1; however, they were characterized by a shorter period of inhibition (<60 msec ISI) and potentiation (60–560 msec ISIs; Fig. 4*C*). Nearly identical paired-pulse–response curves in CA1 or CA3 were obtained with contralateral commissural versus ipsilateral Schaffer collateral (CA1) or mossy fiber (CA3) stimulation. Contralateral stimulation was chosen over ipsalateral for convenience in orientating electrodes. LCMV-infected dentate paired-pulse responses were markedly disinhibited ($p < 0.001$; n = 9) at ISIs <60 msec and slightly disinhibited ($p < 0.02$) at 160–1060 ISIs compared with sham-infected controls (Fig. 4*A*). Although there was no effect in CA3 (Fig. 4*C*; $p > 0.05$; n = 5), LCMV-infected CA1 paired-pulse responses demonstrated slightly decreased ($p < 0.02$; n = 9) paired-pulse potentiation (Fig. 4*B*).

Staining for parvalbumin-containing interneurons

The observed increase in dentate PS amplitudes and the suppression of paired-pulse inhibition in LCMV-infected rats suggested a decrease in GABAergic feedback inhibition, perhaps because of a loss of GABAergic interneurons. Parvalbumin specifically labels a subset of GABAergic interneurons (and their associated neuronal processes) in the hippocampus (Celio, 1990). GABAergic interneurons that contain parvalbumin seem to differentiate late in development (Nitsch et al., 1990) and may be infected with LCMV while the hippocampus is still developmentally immature. We therefore determined whether parvalbumin immunostaining was altered in the dentate gyrus of LCMV-infected rats. The number of parvalbumin-positive cell bodies in the dentate gyrus was quantitated in frozen sections from three infected and three uninfected rats at 79–86 d postinfection. As shown in Figure 5, there is a decrease in parvalbumin-containing neurons and neuronal processes in the dentate gyrus of LCMV-infected rats compared with those of sham-infected controls. The average number of parvalbumin-positive cells in sections from normal dentate gyrus was 5.8 ± 0.93 versus 1.6 ± 1.14 in sections from LCMV-infected brains ($p < 0.05$).

Theta rhythm

EEG activity was recorded from the hilar region of the dentate gyrus of halothane-anesthetized rats. In sham-infected animals, the hippocampal EEG showed infrequent spontaneous episodes of synchronous theta rhythmic activity (3.5–5.5 Hz). Averaged spectral analysis (5 min) revealed mixed frequency activity (Fig. 6). In 10 of 11 LCMV rats tested, the EEG was characterized by constant synchronous theta activity that persisted through the recording session (3–4 hr). In the remaining animal, theta dominated the EEG; however, occasional episodes of mixed activity occurred. The cumulated power spectral analysis of these animals revealed a predominant theta band (Fig. 6). No other distinct power bands (to 60 Hz) were evident under halothane anesthesia. When compared with sham-infected rats, the averaged EEG power spectra in LCMV-infected rats was increased ($p < 0.02$; n = 11) in the theta frequency band (3–5 Hz; resolution = 0.23 Hz) and decreased ($p < 0.02$; n = 11) at lower frequencies (1–3 Hz).

Effects of MK-801 on electrophysiological responses

The NMDA receptor antagonist MK-801 (0.1 $mg \cdot kg^{-1} \cdot d^{-1}$) administered *ad libitum* in the drinking water after weaning had no effect on evoked field potentials, recurrent inhibition, or theta rhythm ($p > 0.05$, n = 4). Notwithstanding a significant ($p < 0.01$) difference in mean weight between LCMV-infected rats and sham-infected rats treated with or without MK-801 [273 ± 4.4 gm (n = 7) vs 322 ± 6.9 gm (n = 9); 84 d postinfection], there seemed to be no differences in fluid consumption or drinking behavior between groups.

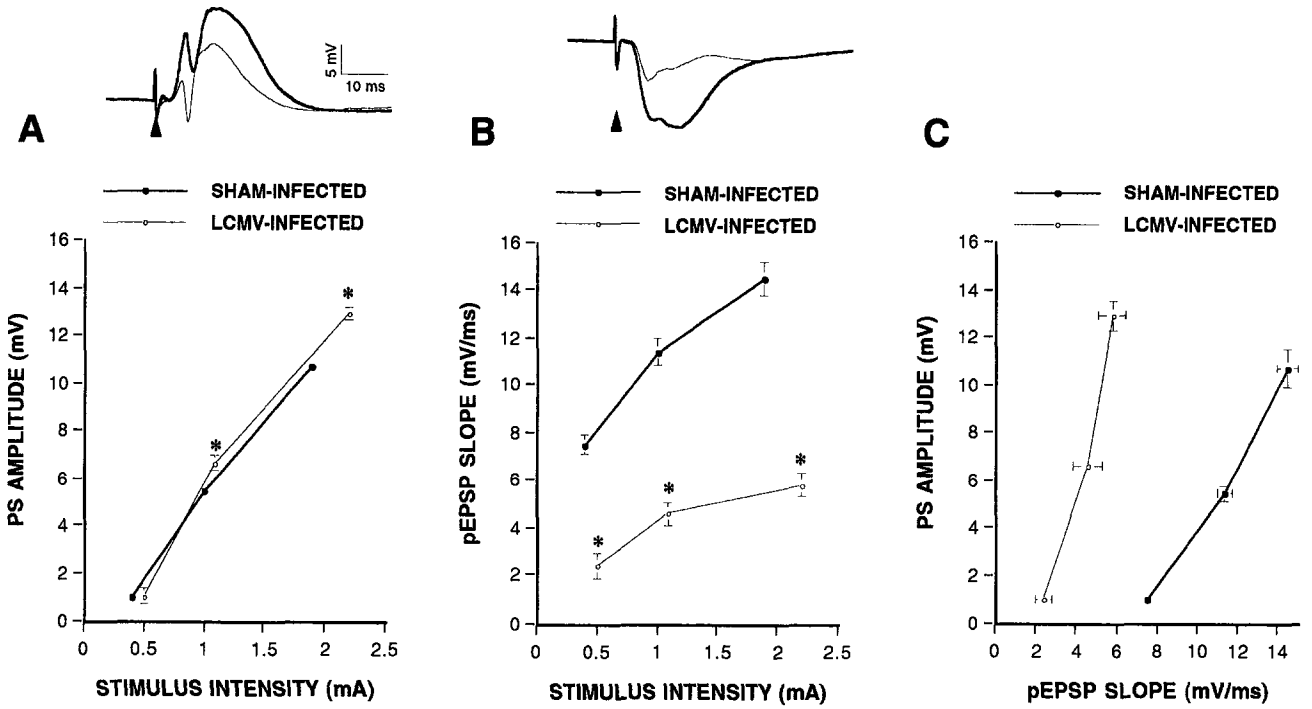

Figure 3. Effects of LCMV infection on dentate gyrus monosynaptic afferent-evoked responses. *A*, *Inset* shows representative superimposed recordings of evoked potentials obtained from the somatic (stratum granulosum) layer of the dentate gyrus in sham-infected and LCMV-infected rats by stimulation of the perforant path (shown here at 50% maximum stimulus level). Somatic recordings were characterized by a fast, negative-going PS on the positive-going pEPSP/IPSP complex waveform and represent the synchronous firing of dentate granule cells. Dentate PS amplitudes increased with increasing stimulus strength and were slightly increased in LCMV-infected rats compared with sham-infected controls. *B*, *Inset* shows representative superimposed recordings of evoked potentials obtained from the dendritic (stratum moleculare) layer of the dentate gyrus in sham-infected and LCMV-infected rats by stimulation of the perforant path (shown here at 50% maximum stimulus level). Dendritic recordings were characterized by a negative-going pEPSP/IPSP complex waveform. The initial deflection on the waveform likely represents a pEPSP. Similar to PS amplitudes, pEPSP slopes increased with increasing stimulus strength but were markedly decreased in LCMV-infected rats compared with sham-infected controls. *Small arrows* indicate stimulus artifact, and *asterisks* represent significance level $p < 0.001$. *C*, A plot of pEPSP slopes at threshold, 50% maximum, and maximum PS amplitude revealed differences in input/output coupling between LCMV-infected rats and their sham-infected controls. The slope of the LCMV curve (3.34 ± 0.7) was significantly steeper than that of controls (1.37 ± 0.17; $p < 0.05$).

DISCUSSION

Although the loss of dentate granule cells was extensive, cell loss did not likely result from direct effects of the virus, as LCMV is relatively noncytopathic to neurons (Rodriquez et al., 1983). Accordingly, granule cell loss in the dentate gyrus continues in adult animals after infectious virus has been cleared (Monjan et al., 1973b, 1974). Nevertheless, some of the cell loss could be attributed to virus-induced destruction or disrupted cell division of precursor cells, which continue to produce new dentate granule cells during the first year of life (Bayer et al., 1982). Although these precursor cells have been estimated to account for as much as a 43% increase in dentate granule cells between 1 month and 1 year of age, even a complete destruction of this population is not adequate to account for the 68–75% loss of dentate granule cells seen 3 months after LCMV infection. Here we report that viral antigens persisted in dentate granule cells long after infectious virus could be detected, but they eventually declined to undetectable levels by 2–3 months postinfection. Considering that hippocampal neuronal circuitry is undergoing developmental changes at the time of the infection (Bayer et al., 1982; Altman and Bayer, 1990) and that functional modulation of neuronal circuitry can lead to neurodegeneration (Sloviter, 1987), it is possible that early virus-induced alterations in hippocampal circuitry may be responsible for the subsequent loss of dentate granule cells.

The increase in PS amplitudes in the dentate gyrus of LCMV-infected rats may result from an enhancement of excitatory transmission or a reduction of GABA-mediated feedforward inhibition of granule cell excitability, or a combination of both. The slope of the pEPSP/PS (E–S) curve indicates that for any given synaptic volley a cellular response is elicited. The E–S potentiation seen in LCMV-infected rats suggests that granule cells are hyperexcitable but may result either from increased postsynaptic excitability or an increase in the ratio of synaptically evoked excitation/inhibition (Wilson et al., 1981; Abraham et al., 1987; Chavez-Noriega et al., 1989). However, the robust suppression of GABA-mediated paired-pulse inhibition observed in LCMV-infected rats provides more definitive support that granule cell hyperexcitability results from decreased recurrent inhibition. Paired-pulse inhibition of monosynaptic afferent-evoked PSs is presumably mediated by GABA interneurons recurrent to principal cells in the dentate gyrus and CA1 as it is suppressed by the $GABA_A$ antagonist bicuculline (Steffensen and Henriksen, 1991). Taken together, these data indicate that although there was a substantial loss of dentate granule cells in the infected rats, those granule cells remaining were receiving enhanced excitatory input. If GABA inhibitory interneurons are more vulnerable to infection and rendered dysfunctional, their subsequent pathology might unleash persistent and pernicious excitatory influences on dentate granule cells.

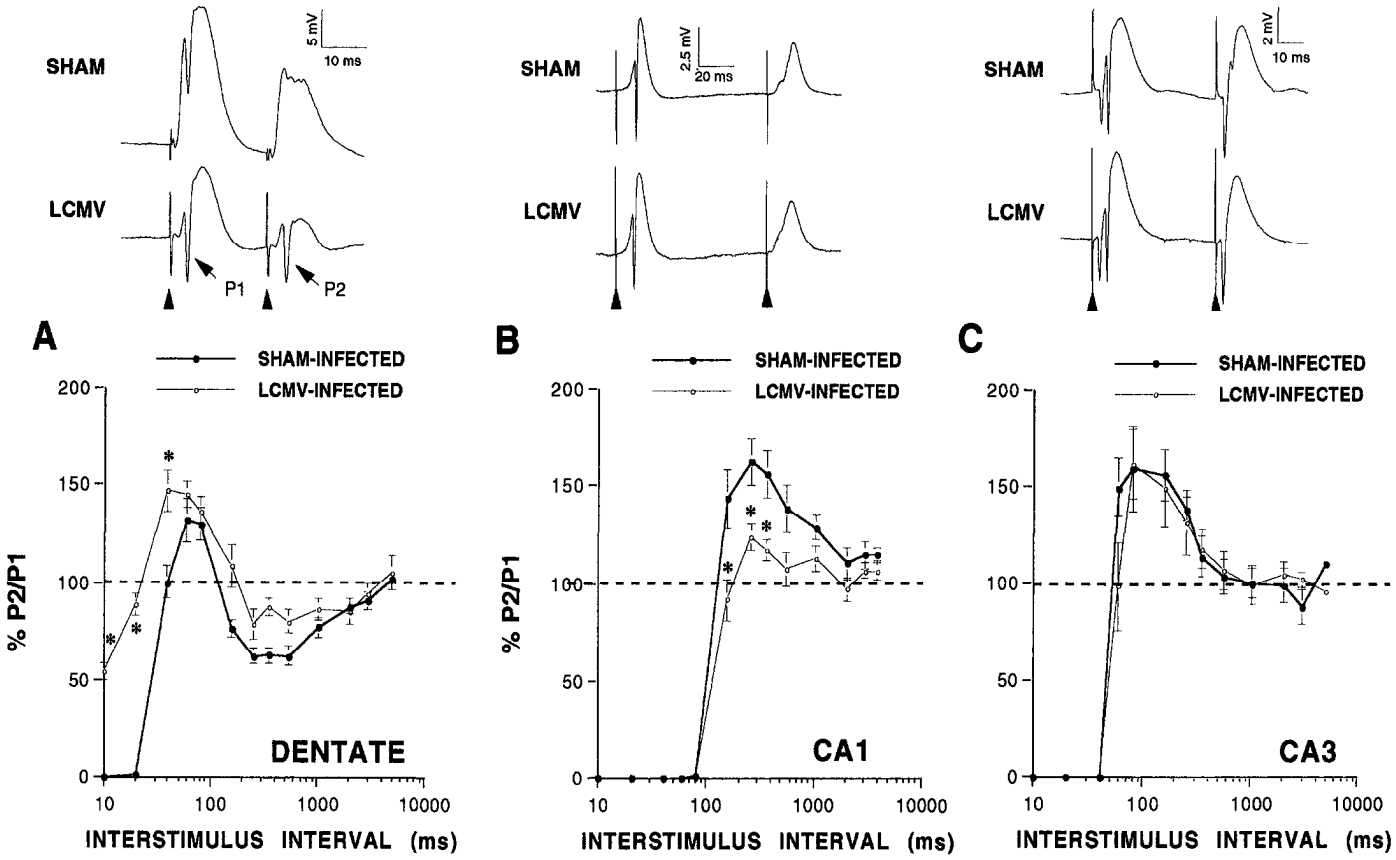

Figure 4. Site-specific effects of LCMV infection on hippocampal recurrent inhibition. *Insets* show representative recordings of waveforms obtained in the dentate gyrus (*A*), CA1 (*B*), and CA3 (*C*) by paired equipotent stimulation of their respective monosynaptic afferents (50% maximum stimulus level). Recurrent inhibition is evidenced in these traces by suppression of the PS amplitude in the conditioned (P2) response at selected ISIs shown for each subfield [20 msec ISI (*dentate*; *A*), 80 msec ISI (*CA1*; *B*), and 40 msec ISI (*CA3*; *C*)]. *Small arrows* indicate stimulus artifacts. Unlike the dentate gyrus and CA1, field responses elicited in CA3 with commissural stimulation were characterized by an early antidromic PS. The second, longer latency PS was determined to be the orthodromic response by the inability to follow high frequency stimuli (200 Hz). *A*, Paired stimuli to the perforant path in sham-infected rats revealed a triphasic response curve [expressed as percentage test PS amplitude (*P2*) vs conditioning PS amplitude (*P1*); see *insets*] of conditioned/test PS amplitudes in the dentate gyrus characterized by absolute inhibition at ISIs below 40 msec, marked potentiation between 40 and 160 msec, and partial inhibition between 0.16 and 4.0 sec ($n = 9$). Paired-pulse inhibition was markedly decreased in the dentate gyrus of LCMV-infected rats ($^*p < 0.001$; $n = 9$). *B*, An increase in paired-pulse inhibition or a decrease in paired-pulse potentiation was evident in the CA1 hippocampal subfield of LCMV-infected rats ($^*p < 0.02$; $n = 9$). *C*, In contrast to the dentate gyrus and CA1, paired-pulse responses were unaffected in the CA3 hippocampal subfield of LCMV-infected rats ($p > 0.05$; $n = 6$).

The role of GABA inhibition in limiting the excitability (Dingledine and Gjerstad, 1980; Miles and Wong, 1987; Stelzer, 1992) and plasticity (Wigstrom and Gustafsson, 1983; Davies et al., 1991) of hippocampal neurons is well known. Notwithstanding the diverse variety of morphologically and immunocytochemically identified neurons characterized in the hippocampus, there are significant parallels between local circuit GABAergic interneuron populations in the dentate gyrus and Ammon's horn. Basket cells in the hippocampus are located in or immediately subjacent to stratum granulosum or stratum pyramidale and contain GABA, as shown by glutamic acid decarboxylase immunocytochemistry (Ribak et al., 1978). A subpopulation of basket cells contains the calcium-binding protein parvalbumin (Kosaka et al., 1987). Electrophysiologically, basket cells in both the dentate gyrus and Ammon's horn as well as interneurons in the hilus or stratum oriens inhibit principal cell excitability by feedforward excitatory input from monosynaptic afferents and by feedback excitatory input from principal cells via axon collaterals (Knowles and Schwartzkroin, 1981).

We found that in the dentate gyrus of LCMV-infected rats, a decreased number of cells and neuronal processes stained for parvalbumin. Parvalbumin is a calcium-binding protein that is thought to protect neurons from damage attributable to the influx of calcium, which can result from the release of excitatory amino acids in pathological conditions (Nitsch et al., 1989; Sloviter, 1989) and is found in a subset of hippocampal GABAergic, probably basket cell, interneurons (Kosaka et al., 1987; Celio, 1990). Some parvalbumin-containing neurons in the dentate gyrus are basket cells that form axosomatic connections on dentate granule cells (Sloviter, 1989). LCMV rats were infected before the developmental stage at which parvalbumin appears (Nitsch et al., 1990). It is not clear whether loss of parvalbumin staining was because of a loss of a specific subpopulation of GABA interneurons or the depletion or change in activity of this protein. Nonetheless, although not cytopathic, LCMV could alter developmental expression of parvalbumin in GABA interneurons and pre-empt its normal protective function against excitotoxicity. Parvalbumin-containing GABA interneurons in the dentate gyrus probably receive excitatory monosynaptic perforant path input and excitatory collaterals from dentate granule cells; therefore, any disruption in inhibitory feedforward or feedback synaptic transmission induced by LCMV infection might lead to profound increases in

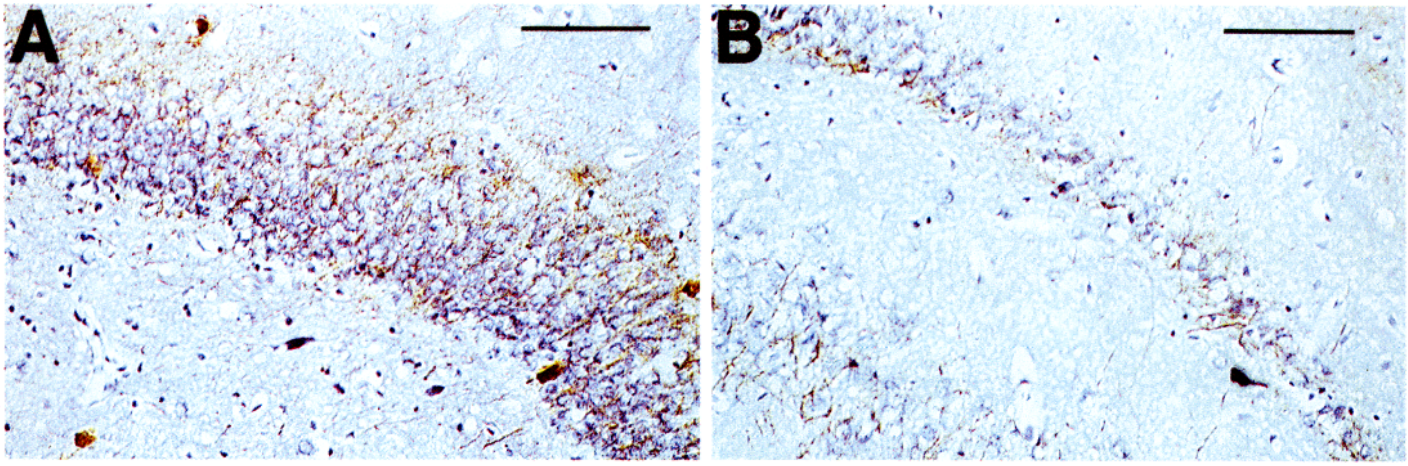

Figure 5. Parvalbumin immunostaining is decreased in the dentate gyrus of LCMV-infected rats. *A*, External limb of the dentate gyrus 83 d after neonatal sham infection demonstrating parvalbumin-containing neurons and neuronal processes in the granule cell layer. *B*, External limb of the dentate gyrus of an LCMV-infected rat at 83 d postinfection showing loss of granule cells and decreased parvalbumin-containing neurons and neuronal processes. Parvalbumin-positive processes are stained brown. Scale bars, 100 μm.

excitatory synaptic transmission. Alternatively, LCMV infection in mice is capable of inhibiting neurotransmitter production (Lipkin et al., 1988), and neurotransmitters in turn help orchestrate the birth and death of neurons during development (Gould et al., 1994). Thus, neonatal infection with LCMV could alter neurotransmitter production, disrupt the developmental program, and indirectly cause dysfunction of inhibitory neurons. Interneurons also could be destroyed as bystanders to the immune response against the virus. GABA interneurons in the dentate gyrus differentiate and migrate prenatally (Amaral and Kurz, 1985; Lubbers et al., 1985) and should be relatively resistant to postnatal LCMV infection; however, cerebellar GABAergic Purkinje cells also form and migrate prenatally, yet they are infected (Altman and Das, 1966; Monjan et al., 1973a; Baldridge et al., 1993). Granule cells are relatively unique in the rat central nervous system in that they evince significant postnatal neurogenesis, with only ~20% of the adult complement of these cells in place at time of birth (Bayer et al., 1982). Although GABAergic interneurons migrate to the dentate gyrus prenatally, these inhibitory cells do not seem to be functionally mature until the third week of postnatal development (Michelson and Lothman, 1989). These findings indicate that the granule cells in the immature rat are under considerably less inhibitory control than those in the mature rat.

The control of hippocampal GABA-mediated inhibition is regulated by remote inputs to the hippocampus (Assaf et al., 1979; Amaral and Cowan, 1980; Krnjevic and Ropert, 1982; Bilkey and Goddard, 1985; Mizumori et al., 1989; Henriksen et al., 1993). Theta rhythm is a prominent EEG pattern generated by the hippocampus, paced by rhythmically firing cells in the medial septum, and characterized by spontaneous 4–10 Hz rhythmic

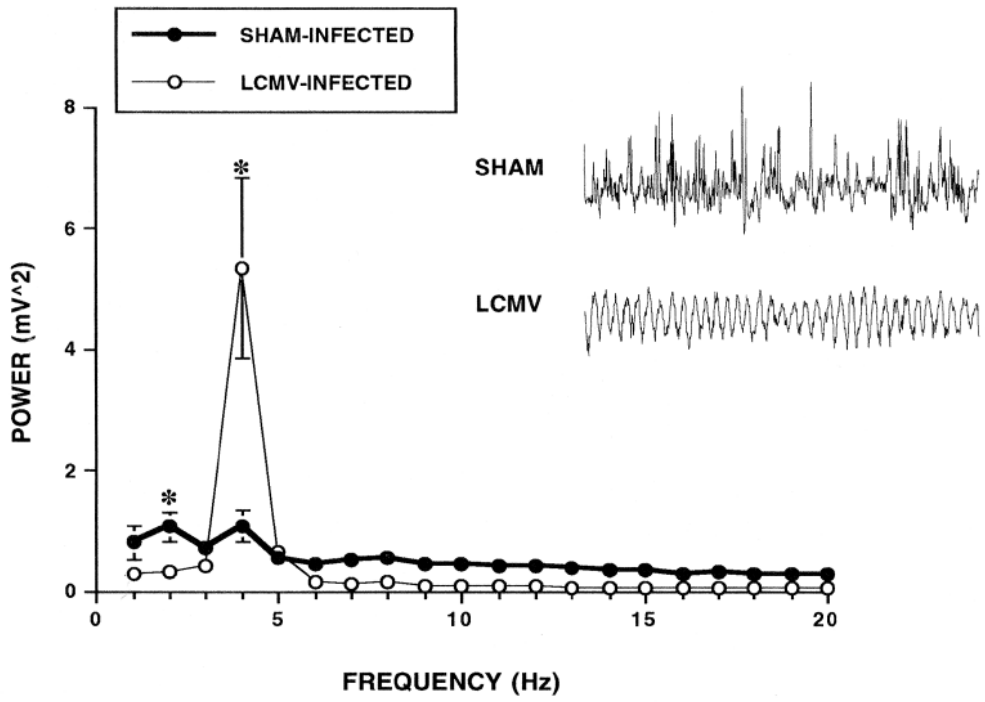

Figure 6. Theta rhythm predominance in LCMV-infected rats. EEG recordings from the dentate hilar region of sham-infected halothane-anesthetized rats were characterized by mixed-frequency activity (*inset* shows 10 sec of raw activity). Averaged spectral analysis (5 min of 4 sec epochs) revealed a shift toward slightly increased power at lower frequencies. The EEGs of LCMV-infected rats were characterized by persistent (maintained during 3–8 hr recording sessions) synchronous rhythmic activity that evinced a 3–5 Hz theta power band with spectral analysis. The theta band of LCMV-infected rats was increased and the 1–3 Hz band was decreased compared with those of sham-infected controls. *Asterisks* represent significance levels $p < 0.02$.

activity in freely behaving animals (Stewart and Fox, 1990). The hippocampal EEG of LCMV-infected rats was dominated by persistent theta, suggesting that septohippocampal input to the hippocampus is dysfunctional or that hippocampal target neurons respond anomalously to the rhythmic pacemaker activity. Inasmuch as there was no evidence for neurodegeneration in the septum, the latter hypothesis is more convincing in light of the histopathological findings in the dentate gyrus.

If NMDA receptor-mediated excitotoxicity is the final insult responsible for the pathological changes in LCMV-infected rats, we would expect that the NMDA antagonist MK-801 might prevent these changes. Treatment of rats with MK-801 had no effect on the cell loss or on any of the abnormal electrophysiological measures found in LCMV-infected rats. It has been demonstrated that MK-801 treatment effectively protects against measles virus-induced CA1 hippocampal neurodegeneration, suggesting possible NMDA receptor involvement in viral excitotoxicity. The lack of effect of MK-801 on the granule cell loss and hyperexcitability in the dentate gyrus of LCMV-infected rats may be attributed to differences in the methodologies used. In the measles study, adult mice were used, the dose of MK-801 was greater, the duration of treatment was shorter, and the effective window of time for protection was determined to be 4–7 d postinoculation (Andersson et al., 1993). In this study, MK-801 was not administered until the animals were weaned and after infectious virus had been cleared from the animals; therefore, we may have missed the window of maximally effective protection. Alternatively, cell death associated with LCMV infection could be mediated by non-NMDA excitatory amino acid receptors.

This study clarifies the long-term pathophysiological changes in the hippocampus that result from neonatal infection with LCMV and suggests a novel mechanism by which a viral infection early in postnatal development can lead to neurodegeneration in the absence of residual viral gene products. Given the importance of the hippocampus in learning and memory, and its potential role in neurodevelopmental disorders, additional studies are warranted to determine the behavioral consequences of viral infection and to determine the precise mechanism by which dentate granule cells are destroyed. These studies will provide clues as to how perinatal viral infection in humans can lead to neuropsychiatric and developmental disorders.

REFERENCES

Abraham WC, Gustaffson B, Wigstrom H (1987) Long-term potentiation involves enhanced synaptic excitation relative to synaptic inhibition in guinea-pig hippocampus. J Physiol (Lond) 394:367–380.

Altman A, Bayer SA (1990) Migration and distribution of two populations of hippocampal granule cell precursors during the perinatal and postnatal periods. J Comp Neurol 301:365–381.

Altman J, Das GD (1966) Autoradiographic and histological studies of postnatal neurogenesis. I. A longitudinal investigation of the kinetics, migration and transformation of cells incorporating tritiated thymidine in neonate rats, with special reference to postnatal neurogenesis in some brain regions. J Comp Neurol 126:337–390.

Amaral DG, Cowan WM (1980) Subcortical afferents to the hippocampal formation in the monkey. J Comp Neurol 189:573–591.

Amaral DG, Kurz J (1985) The time and origin of cells demonstrating glutamic acid decarboxylase-like immunoreactivity in the hippocampal formation of the rat. Neurosci Lett 59:33–39.

Andersson T, Schwarcz R, Love A, Kristensson K (1993) Measles virus-induced hippocampal neurodegeneration in the mouse: a novel, subacute model for testing neuroprotective agents. Neurosci Lett 154:109–112.

Assaf SY, Mason ST, Miller JJ (1979) Noradrenergic modulation of neuronal transmission between the entorhinal cortex and the dentate gyrus of the rat. J Physiol (Lond) 292:52P.

Baldridge JR, Pearce BD, Parekh BS, Buchmeier MJ (1993) Teratogenic effects of neonatal arenavirus infection on the developing rat cerebellum are abrogated by passive immunotherapy. J Virol 197:669–677.

Bauman M (1991) Microscopic neuroanatomic abnormalities in autism. Pediatrics [Suppl] 87:791–796.

Bayer SA, Yackel JW, Puri PS (1982) Neurons in the rat dentate gyrus layer substantially increase during juvenile and adult life. Science 216:890–892.

Bilkey DK, Goddard GV (1985) Medial septal facilitation of hippocampal granule cell activity is mediated by inhibition of inhibitory interneurons. Brain Res 361:99–106.

Bogerts B (1993) Recent advances in the neuropathology of schizophrenia. Schizophr Bull 19:431–445.

Celio MR (1990) Calbindin D-28 and parvalbumin in the rat nervous system. Neuroscience 35:375–474.

Chavez-Noriega LE, Bliss TVP, Halliwell JV (1989) The EPSP-spike (E–S) component of long-term potentiation in the rat hippocampal slice is modulated by GABAergic but not cholinergic mechanisms. Neurosci Lett 104:58–64.

Davies CH, Starkey SJ, Pozza MF, Collingridge GL (1991) $GABA_B$ autoreceptors regulate the induction of LTP. Nature 349:609–611.

Deykin EY, MacMahon B (1979) Viral exposure and autism. Am J Epidemiol 109:628–638.

Dingledine R, Gjerstad L (1980) Reduced inhibition during epileptiform activity in the in vitro hippocampal slice. J Physiol (Lond) 305:297–313.

Gould E, Cameron HA, McEwen BS (1994) Blockade of NMDA receptors increases cell death and birth in the developing rat dentate gyrus. J Comp Neurol 340:551–565.

Henriksen SJ, Steffensen SC, Criado JR (1993) Facilitation of dentate gyrus field responses by VTA stimulation is attenuated by dopamine antagonists. Soc Neurosci Abstr 19:1374.

Houser CR (1990) Granule cell dispersion in the dentate gyrus of humans with temporal lobe epilepsy. Brain Res 535:195–204.

Kirch DG (1993) Infection and autoimmunity as etiologic factors in schizophrenia: a review and reappraisal. Schizophr Bull 19:355–370.

Knowles WD, Schwartzkroin PA (1981) Local circuit interactions in hippocampal brain slices. J Neurosci 1:318–322.

Kosaka T, Katsumaru H, Hama K, Wuy JY, Heizmann CW (1987) GABAergic neurons containing the calcium binding protein parvalbumin in the rat hippocampus and dentate gyrus. Brain Res 419:119–130.

Krnjevic K, Ropert N (1982) Electrophysiological and pharmacological characteristics of facilitation of hippocampal population spikes by stimulation of the medial septum. Neuroscience 7:2165–2183.

Lipkin WI, Battenberg ELF, Bloom FE, Oldstone MBA (1988) Viral infection of neurons can depress neurotransmitter mRNA levels without histologic injury. Brain Res 451:333–339.

Lubbers K, Wolff JR, Frotscher M (1985) Neurogenesis of GABAergic neurons in the rat dentate gyrus: a combined autoradiographic and immunocytochemical study. Neurosci Lett 62:317–322.

Margolis G, Kilham L (1975) Problems of human concern arising from animal models of intrauterine and neonatal infections due to viruses: a review. Prog Med Virol 20:144–179.

Michelson HB, Lothman EW (1989) An in vivo electrophysiological study of the ontogeny of excitatory and inhibitory processes in the rat hippocampus. Dev Brain Res 47:113–122.

Miles R, Wong RKS (1987) Inhibitory control of local excitatory circuits in the guinea-pig hippocampus. J Physiol (Lond) 388:611–629.

Mizumori SJY, McNaughton BL, Barnes CA (1989) A comparison of supramammillary and medial septal influences on hippocampal field potentials and single-unit activity. J Neurophysiol 61:15–31.

Monjan AA, Bohl LS, Hudgens GA (1975) Neurobiology of LCMV virus in rodents. Bull WHO 52:487–491.

Monjan AA, Cole GA, Gilden DH (1973a) Pathogenesis of cerebellar hypoplasia produced by lymphocytic choriomeningitis virus infection of neonatal rats. I. Evolution of disease following infection at 4 days of age. J Neuropathol Exp Neurol 32:110–124.

Monjan AA, Cole GA, Nathanson N (1973b) Pathogenesis of LCMV disease in the rat. In: Lymphocytic choriomeningitis virus and other arenaviruses (Lehmann-Grube F, ed), pp 195–206. New York: Springer.

Monjan AA, Cole GA, Nathanson N (1974) Pathogenesis of cerebellar hypoplasia produced by lymphocytic choriomeningitis virus infection of neonatal rats: protective effect of immunosuppression with anti-lymphoid serum. Infect Immun 10:449–502.

Nadler JV, Perry BW, Cotman CW (1978) Intraventricular kainic acid preferentially destroys hippocampal pyramidal cells. Nature 27:676–677.

Narayan O, Herzog S, Frese K, Scheefers H, Rott R (1983) Pathogenesis of Borna disease in rats: immune-mediated viral ophthalmoencephalopathy causing blindness and behavioral abnormalities. J Infect Dis 148:305–315.

Nitsch R, Bergman I, Kuppers K, Mueller G, Frotscher M (1990) Late appearance of parvalbumin-immunoreactivity in the development of GABAergic neurons in the rat hippocampus. Neurosci Lett 118: 147–150.

Nitsch C, Scotti A, Sommacal A, Kalt G (1989) GABAergic hippocampal neurons resistant to ischemia-induced neuronal death contain the Ca^{2+}-binding protein parvalbumin. Neurosci Lett 105:263–268.

Oldstone MA, Rodriguez M, Daughaday WH, Lampert PW (1984) Viral perturbation of endocrine function: disordered cell function leads to disturbed homeostasis and disease. Nature 307:278–281.

Olney JW, Labruyere J, Wang G, Wozniak DF, Price MT, Sesma MA (1991) NMDA antagonist neurotoxicity: mechanism and prevention. Science 254:1515–1518.

Parham D, Tereba A, Talbot PJ, Jackson DP, Morris VL (1986) Analysis of JHM central nervous system infections in rats. Arch Neurol 43:702–708.

Prober CG, Arvin AM (1987) Perinatal viral infection. Eur J Clin Microbiol 6:245–261.

Ribak C, Vaughn J, Saito K (1978) Immunocytological localization of glutamic acid decarboxylase in neuronal somata following colchicine inhibition of axonal transport. Brain Res 140:315–322.

Rodriquez M, Buchmeier MJ, Oldstone MBA, Lampert PW (1983) Ultrastructural localization of viral antigens in the CNS of mice persistently infected with lymphocytic choriomeningitis virus (LCMV). Am J Virol 110:95–100.

Sloviter RS (1987) Decreased hippocampal inhibition and a selective loss of interneurons in experimental epilepsy. Science 235:73–76.

Sloviter RS (1989) Calcium-binding protein (Calbindin-D28k) and parvalbumin immunocytochemistry: localization in the rat hippocampus with specific reference to the selective vulnerability of hippocampal neurons to seizure activity. J Comp Neurol 280:183–196.

Steffensen SC, Henriksen SJ (1991) Effects of baclofen and bicuculline on inhibition in the fascia dentata and hippocampus regio superior. Brain Res 538:46–53.

Stelzer A (1992) $GABA_A$ receptor populations control the excitability of neuronal populations. Int Rev Neurobiol 33:195–287.

Stewart M, Fox SE (1990) Do septal neurons pace the hippocampal theta rhythm? Trends Neurosci 3:163–169.

Stoltenburg G, Schmidt S, Marzheuser S, Herbst H, Spiegel H, Unger M (1991) The central nervous system of infants born to HIV-positive mothers: neuropathology, immunohistochemistry in in situ hybridization. Verh Dtsch Ges Pathol 75:191–194.

Wigstrom H, Gustafsson JB (1983) Facilitated induction of long-lasting potentiation during blockade of inhibition. Nature 301:603–605.

Wilson RC, Levy WB, Steward O (1981) Changes in translation of synaptic excitation to dentate granule cell discharge. II. An evaluation of mechanisms utilizing dentate gyrus dually innervated by surviving ipsilateral and sprouted crossed temporodentate inputs. J Neurophysiol 46:339–355.